Article:

Mohsenian, V. orcid.org/0000-0002-5918-1569, Gharaei-Moghaddam, N. orcid.org/0000-0003-3309-2864 and Hajirasouliha, I. orcid.org/0000-0003-2597-8200 (2022) An innovative variable target time method for probabilistic-based seismic performance assessment of multi-storey buildings. Journal of Building Engineering, 52. 104378. ISSN: 2352-7102

https://doi.org/10.1016/j.jobe.2022.104378

Journal of Building Engineering 52 (2022) 104378

Contents lists available at ScienceDirect

Journal of Building Engineering

journal homepage: www.elsevier.com/locate/jobe

An innovative variable target time method for probabilistic-based seismic performance assessment of multi-storey buildings

Vahid Mohsenian [a,*], Nima Gharaei-Moghaddam [b], Iman Hajirasouliha [c]

[a] Department of Civil Engineering, University of Science and Culture, Tehran, Iran
[b] Department of Civil Engineering, Ferdowsi University of Mashhad, Mashhad, Iran
[c] Department of Civil and Structural Engineering, The University of Sheffield, Sheffield, UK

ARTICLE INFO

Keywords:
Endurance time analysis
Incremental dynamic analysis
Reliability analysis
Fragility curves
IM-Based method
EDP-Based method

ABSTRACT

Incremental dynamic analysis is one of the most widely used methods to develop fragility curves due to its ability to deal with various inherent uncertainties in the prediction of earthquake recurrence and characteristics. The dependence of the results to the selected ground motion records, uncertainties associated with the selection of appropriate earthquake input records and high computational costs are among the challenges limit the practical applications of this method. In this study, an innovative variable target time (VTT) method is developed based on the concept of endurance time (ET) analysis for structural reliability assessment of 3D multi-storey structures. A novel low-computational cost process is proposed to develop the database of desired statistical population and estimate the probabilities for constant hazard levels (EDP-based method) by taking into account the uncertainties in the frequency content of the input earthquakes. To verify the accuracy of the outcomes, the results are compared with the fragility curves derived based on different damage levels (IM-based method) and Incremental Dynamic Analysis (IDA) for moment-resisting steel and tunnel-from concrete 3D structures with 5- and 10-storeys. The results indicate that the proposed method is capable of providing highly accurate probabilistic models for structural performance under different levels of earthquake intensity. For the selected steel moment-resisting structures, the maximum difference in the reliability results obtained by the two methods of analysis for the Immediate Occupancy (IO), Life Safety (LS), and Collapse Prevention (CP) performance levels under the Design Basis Earthquake (DBE) and the Maximum Considered Earthquake (MCE) are around 2, 7 and 5%, respectively. Similarly, the reliability results for the 3D tunnel-from concrete structures show around 6, 7, and 6% errors between the two analysis methods for the IO, LS and CP performance levels, respectively. The proposed method reduces the computational costs of the IDA-based methods by 80%, and hence, can be considered as a suitable alternative for the conventional methods to develop fragility curves of 3D structures.

1. Introduction

Due to various uncertainties in structural performance evaluation, application of probabilistic methods to assess the seismic performance of structural systems at different hazard levels has attracted significant interest in the past decades [1]. In practical

* Corresponding author.
E-mail address: v.mohsenian@usc.ac.ir (V. Mohsenian).

https://doi.org/10.1016/j.jobe.2022.104378
Received 9 November 2021; Received in revised form 13 February 2022; Accepted 14 March 2022
Available online 17 March 2022

applications, instead of definitively expressing a level of intensity that causes a particular damage level in the system, it is generally preferred to determine the probabilistic distribution of the response corresponding to a given damage level for different levels of intensity (IM-Based Method). As an alternative approach, the probabilistic distribution of structural response can be also presented for a given intensity of applied stimulation (EDP-Based Method) [2,3].

One of the common methods for seismic performance evaluation of structures is fragility analysis. In general, the fragility curves represent the cumulative probability of damages and can be defined as follows [4].

$$Fragility = P[r \geq R | IM = im] \tag{1}$$

where *r* represents the structural response, *R* stands for a limit state corresponding to a certain damage level, *IM* is earthquake intensity measure and *im* is a specific intensity of excitation. Extraction of fragility curves requires statistical and probabilistic studies. Depending on the desired level of accuracy, different methods such as expert judgement-based methods, statistical empirical methods, experimental methods, analytical methods, and combined methods can be adopted for development of fragility curves. Currently, in most seismic vulnerability studies, analytical methods are utilized. Among the existing analytical approaches, incremental dynamic analysis (IDA) is of paramount importance due to the desired accuracy and its capability in dealing with the inherent uncertainties regarding future earthquakes [5]. In this analytical approach, different ground motion records with properties close to the site conditions are selected to investigate the effects of different earthquake parameters on the seismic response of the structure. After choosing the appropriate intensity (IM) and damage (DM) measures, the intensity of the scaled accelerograms is increased incrementally and the resulting excitations are applied to the structure. At each step, the structural response is recorded. Subsequently, the IDA curves are developed by plotting the relationship between intensity and damage measures for each accelerogram (see Fig. 1).

To derive fragility curves for a given performance level (IM-Based Method) using IDA, the following steps must be followed:

1. According to Fig. 1 (a), the intensity measure corresponding to a certain level of damage (or performance level) in the system is extracted from each of the IDA curves.
2. Assuming the log-normal distribution for the attained values in the previous step, the mean, μ, and standard deviation, σ, parameters are computed and the values of the probability density function for the considered performance level are calculated using the following equation:

$$f(x) = \frac{1}{\sigma\sqrt{2\pi}} EXP\left(\frac{(x-\mu)^2}{-2\sigma^2}\right) \tag{2}$$

3. According to Fig. 1, considering x_0 as a particular intensity, the area under the probability density function from -∞ to x_0 gives the probability of exceeding the desired damage level (P). This means that at this particular intensity, there is a probability of P that structural response exceeds the response corresponding to the desired damage (or performance) level.
4. The reliability of the structure for the desired damage (or performance) level, P_0, is derived by subtracting P from 1. It means that at the given earthquake intensity level, x_0, there is a probability of P_0 that the structure will not experience the corresponding performance level.

Fragility analysis can also be performed for a given intensity level (EDP-Based Method). In this method, there is no need to perform full IDA, and using a set of accelerograms scaled to a specific intensity will be sufficient. To extract the fragility curves in this method the following steps are used:

1. According to Fig. 1 (b), the accelerograms scaled to a specific intensity are applied to the structure and the structural responses corresponding to each accelerogram are recorded.

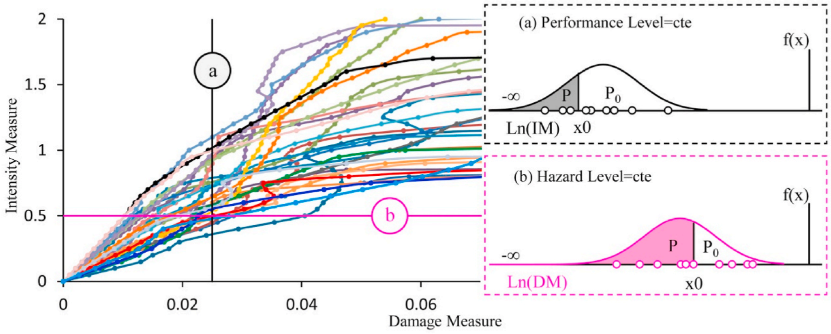

Fig. 1. Fragility analysis using IDA results (a) The probability of exceeding a certain performance level under the desired intensity (x_0); (b) Reliability of the system for the performance level (x_0) under a given intensity level [2].

2. Assuming the log-normal distribution for the attained values in the previous step, the mean, μ, and standard deviation, σ, of the responses are computed and the values of the probability density function for the considered performance level are calculated using Eq. (2).
3. According to Fig. 1, considering x_0 as a particular response, the area under the probability density function from -∞ to x_0 provides the probability, P, that the structural response does not exceed the considered response, x_0.
4. Similar to the previous method, the fragility of the structure for the considered response, P_0, is derived by subtracting P from 1.

Fragility analysis has been widely used for assessing the seismic vulnerability of different structural systems. For example, Mohsenian and Mortezaei [6] developed fragility curves to study the seismic vulnerability of tunnel-form structures. In a more recent study, Mohsenian and Nikkhoo [7] and Mohsenian et al. [8], utilized fragility analysis to investigate the effect of irregularities on seismic performance of tunnel-form structures. Mohsenian et al. [9] also evaluated the reliability of high-rise structures with the diagrid system using the EDP-based method. Banerjee and Chi [10] used fragility analysis to perform a vulnerability assessment of bridges under external loads. In this study, the authors utilized the results of time history analysis for the development of fragility curves. In another relevant study, Mohsenian et al. [11,12] performed fragility and reliability analysis to assess the influence of vertical links on improving the seismic performance of weak moment-resisting frame structures.

Grigoriu [13] showed that development of fragility curves for multi-degrees of freedom structures using spectral acceleration as the intensity measure, which is a common practice, may lead to large uncertainties. Koutsourelakis [14] also suggested the application of the Bayesian framework to develop multi-dimensional fragility surfaces for seismic vulnerability evaluation of structures. Similarly, Wang and Lyons [15] investigated the potential of the large-sample normal approximation to Bayesian posterior distributions in linear seismic fragility analysis. Olmati et al. [16] utilized fragility analysis for performance-based design of cladding wall panels subjected to blast loading. In a recent study, Xiang et al. [17] utilized fragility seismic analysis to investigate the effect of shape memory alloys on the performance of concrete bridge piers. In an attempt to apply fragility analysis for assessment of structures performance under

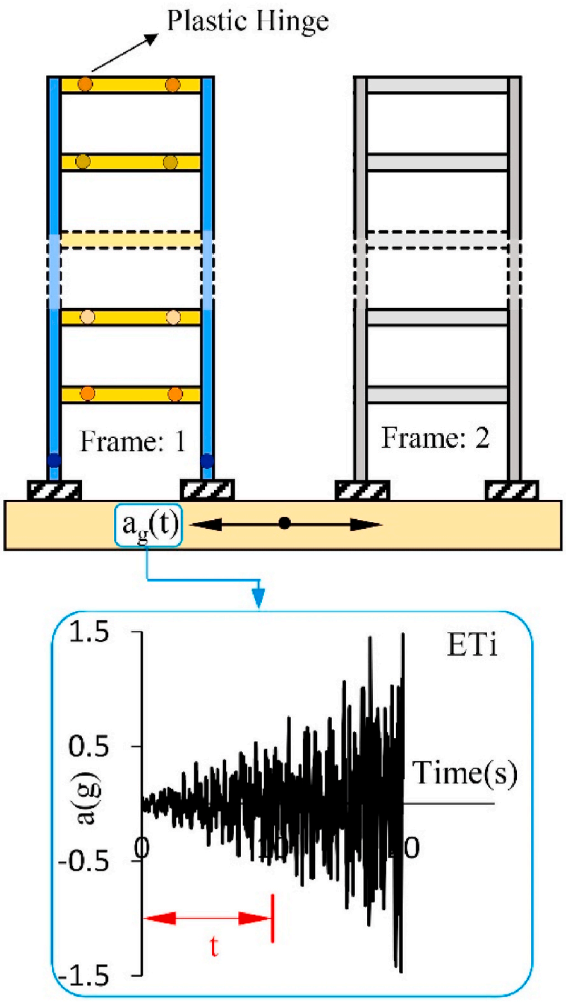

Fig. 2. Schematic representation of endurance time analysis on two structures.

seismic sequences, Kalantari and Roohbakhs [18] developed fragility curved for code-conforming reinforced concrete moment resisting frames damaged by mainshocks. Pang et al. [19] also performed fragility analysis to study the effect of mainshock-aftershock sequence on seismic performance of a high concrete face rockfill dam considering plastic failure effects.

One of the recent applications of fragility analysis for seismic assessment of arch dams is performed by Liang et al. [20] who developed the fragility curves considering different failure modes of the arch dam-foundation system. Recently, various researchers attempted to utilize soft computing approaches as well as machine learning methods to facilitate the development of fragility curves for different types of structures [21,22].

The proper selection of accelerograms as well as the intensity and damage measures are the key parameters affecting the accuracy of IDA results. In a statistical study, in addition to the above-mentioned issues, the number of accelerograms is also important. In general, as the number of ground motion records increases, the uncertainties associated with the earthquake decrease. However, by increasing the number of accelerograms, the computation time and efforts for nonlinear analysis also increases significantly, which is a challenge in utilizing this method. To address some of the existing challenges of IDA based methods, researchers have proposed several strategies including using push-over analyses with complex backbone shapes [23], modal push-over analysis [24], and the modified N2 method [25]. This highlights the need for the development of high-precision analytical methods, which could provide accurate fragility curves while reducing the computational effort, as an alternative for the current IDA-based methods. The recently developed endurance time method seems to be a possible alternative to achieve this goal.

The endurance time (ET) analysis is a novel structural analysis approach, in which a specific record with increasing acceleration amplitude is applied to the structure (see Fig. 2) [26,27]. In this method, the strength criterion is the time until which the structure remains stable under the applied increasing acceleration excitation (target time *t*). Applying an accelerating acceleration function until time *t* is equivalent to use a design earthquake with a certain return period. The maximum responses of the structure at the time *t* are then compared with the allowable design values under the considered hazard level (see Fig. 3). For instance, for the two hypothetical frames shown in Fig. 2, and after calculating their responses as illustrated in Fig. 3, it is expected that frame No. 2 exhibits better seismic performance compared to frame No. 1 under the hazard level corresponding to time *t*.

Several studies have been performed on the applications of endurance time analysis and demonstrated the good agreement between its results and the outcomes of static and spectrum analysis [28,29]. In some of the previous studies, the endurance time method has been also used for analysis of non-building structures such as offshore platforms [30,31]. Shirkhani et al. [32] utilized the endurance time method for seismic performance analysis of steel frame structures equipped with rotational friction dampers. In another relevant study, Hariri-Ardebili et al. [33] suggested a new type of damage and performance indices for concrete arch dams using endurance time analysis. Foyouzat and Estekanchi [34] also proposed the application of nonlinear rigid-perfectly plastic spectra, instead of linear elastic spectra, to correlate the seismic hazard return period and the time in the endurance time analysis.

Gou et al. [35] utilized the endurance time analysis to investigate seismic-induced pounding of highway bridges. Bai et al. [36] adopted the endurance time method for seismic performance evaluation of steel plate shear wall systems. They found that the endurance time approach can produce highly accurate estimations with considerably lower computational efforts in comparison with other common analytical techniques. In another recent study, Bai et al. [37] investigated the soil-structure interaction response of reinforced concrete frame structures using endurance time method.

It should be noted that the common methods for simulating excitations in the endurance time analysis generally consider only the amplitude and the frequency content of the input ground motions. This indicates that the parameters regarding cumulative damage of structures may be neglected. To address this issue, Mashayekhi et al. [38] proposed a new simulation process for the endurance time excitation, which results in improved hysteretic energy compatibility with ground motions.

Mohsenian et al. [39] suggested using the endurance time method for multi-level estimation of response modification factors. In another study, Mohsenian et al. [40] proposed a new analysis scenario based on the endurance time approach for estimating the remaining capacity of structures subjected to ground motions sequences.

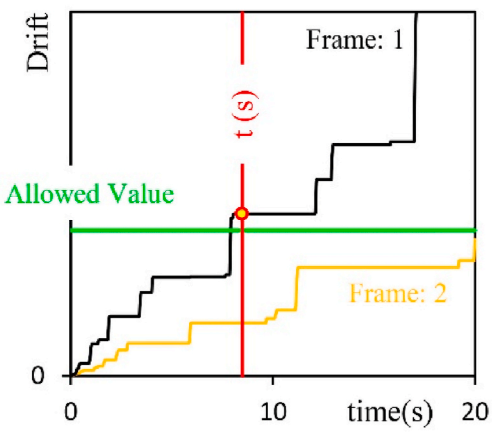

Fig. 3. Variation of damage indices for the assumed structures in the endurance time analysis.

As discussed in the previous section, the dependence of the results of time history analysis to the frequency content of the selected ground motion records, the considerable variety of the available accelerograms and the issues related to their proper selection, as well as high computational costs are some of the main challenges for the application of nonlinear time history analysis in conventional fragility analysis methods. These issues highlight the need for an alternative analytical approach that can provide accurate and reliable results with lower computational time and effort.

The main objective of this study is to develop a low computational cost approach, as a practical alternative to the conventional IDA based methods, to perform reliability analyses and develop fragility curves in 3D multi-storey buildings by using the concept of ET analysis. The main difference of the present method with previous studies on ET is the adoption of the constant hazard approach (EDP-based method) for developing the statistical population required to obtain the fragility curves. A novel approach, called variable target time (VTT), is also proposed to take into account the uncertainties in the frequency content of the input earthquakes in the ET method by using different scale factors. The efficiency of the proposed method is then evaluated for both steel moment-resisting and tunnel-from concrete 3D buildings with 5- and 10-storeys.

2. Application of the VTT method for moment-resisting steel structures

2.1. Selected moment-resisting steel structures

In this section, 3D intermediate moment-resisting steel structures (IMF) with the plan shown in Fig. 4 are selected. The floor system is considered to be reinforced concrete, with dead loads (Q_D) and live loads (Q_L) equal to 630 and 200 kgf/m^2, respectively (roof live load is 150 kgf/m^2). According to the figure, the span length and storey height are 5 and 3.2 m, respectively. To investigate the effect of height on the performance of structures, 5- and 10-storey structures are considered. The structures are assumed to be residential buildings located on a site with high seismic hazard (PGA = 0.35 g) and soil class type C according to ASCE7 [41] (shear wave velocity ranging from 375 to 750 m/s). The properties of the beam and column sections are provided in Table 1 with the notations shown in Fig. 5. Since the beam sections are similar at each storey level, and the columns are symmetrical with respect to the vertical axis (see Fig. 4), only part of the frame is demonstrated in Fig. 5. The effect of the rigid diaphragms is included in the developed models. The mild steel with a yield stress of 240 MPa and a Poisson ratio of 0.3 is considered for the structures. It should be noted that the studied structures are designed according to AISC360-2010) [42] using ETABS software [43].

2.2. Nonlinear modeling approach

In this study, PERFORM-3D software [44] is used for nonlinear modeling and analysis of the structures. Due to the assumption of the rigid beam to column connections in the studied structures, nonlinear behavior is considered only at two ends of the beam and column elements (i.e. critical locations susceptible to formation of plastic hinges). The generalized force-deformation curve depicted in Fig. 6 is used to model beams and columns in the software. Parameters a, b and c in this figure are taken from the table of modeling and acceptance criteria in nonlinear methods for steel components of ASCE/SEI41-17 [45].

In Fig. 6, the maximum expected strength, Q_{CE}, for beams and columns is derived using Eqs. (3) and (4), respectively. In these

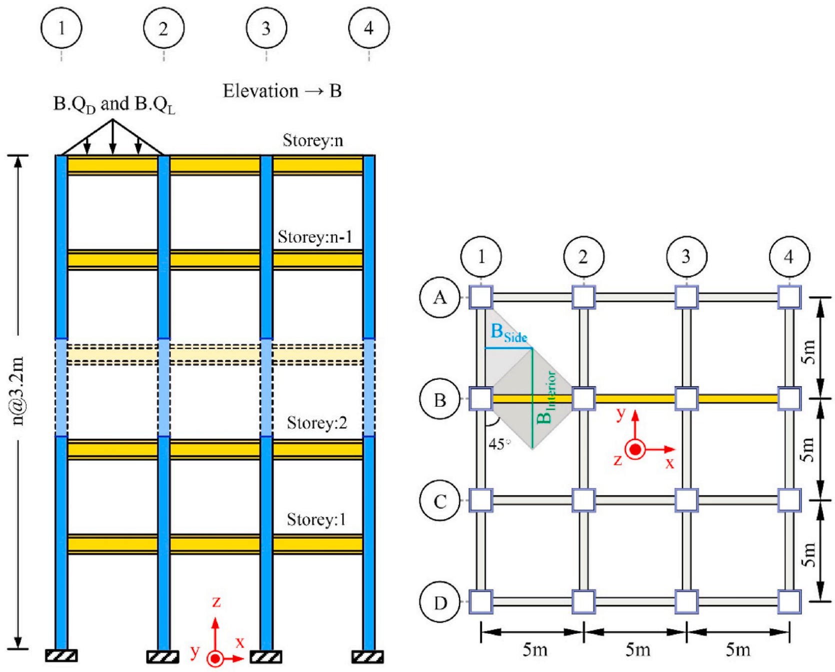

Fig. 4. Loading area of the exterior and interior beams in the plan of the studied moment-resisting steel structures and a schematic view of a frame.

Table 1
Beam and column section properties (dimensions are in millimeters).

Columns		Beams	
ID	Section (B.t)	ID	Section (H_w.t_w-B_f.t_f)
C_0	500.20	B_0	300.10–150.20
C_1	400.15	B_1	300.10–150.15
C_2	300.15	B_2	300.15–180.15
C_3	250.15	B_3	350.10–250.25
C_4	200.15	B_4	350.10–200.25
C_5	350.15	B_5	270.10–180.20
C_6	400.20	B_6	240.10–150.20
C_7	300.20	B_7	270.10–150.20
C_8	200.20	B_8	200.10–150.15
C_9	270.15	B_9	350.10–180.20
C_{10}	240.15	B_{10}	350.10–200.20
–	–	B_{11}	300.10–200.20

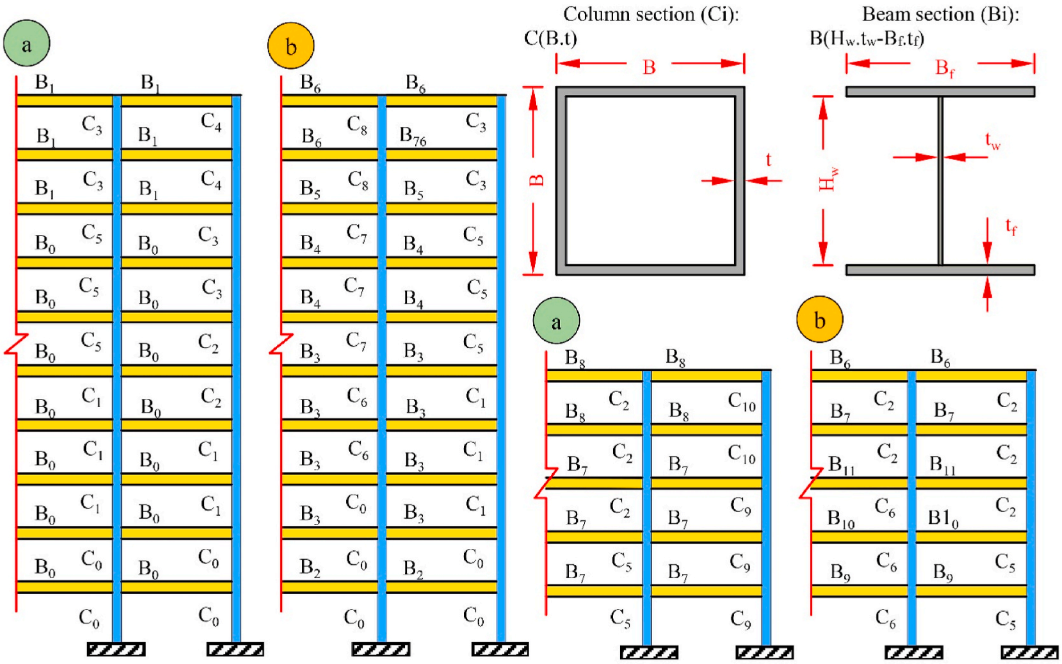

Fig. 5. Geometric properties of the studied moment-resisting steel structures (a) External Frames (1, 4, A, and D); (b) Internal Frames (2, 3, B, and C).

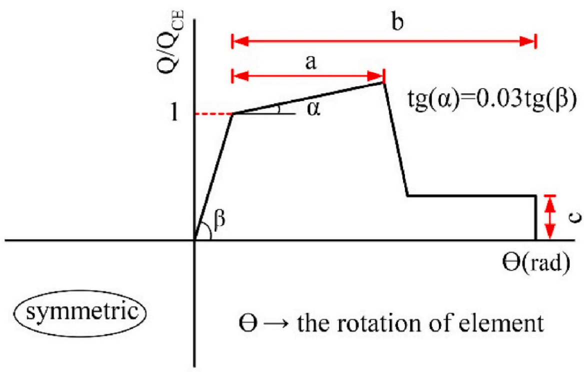

Fig. 6. Force-deformation curve for steel components (adapted from Ref. [45]).

equations, Z and F_{ye} are the plastic section modulus and the expected yield stress of the utilized steel material, respectively. P is the axial force of the member at the beginning of the dynamic analysis, while P_{ye} represents the expected yield axial force of the member calculated as the product of the cross-section area A and the expected yield stress of the materials.

$$Q_{CE} = Z.F_{ye} \tag{3}$$

$$Q_{CE} = Z.F_{ye}\left(1-\frac{|P|}{2P_{ye}}\right) i\left(\frac{|P|}{2P_{ye}}<0.2\right) \tag{4}$$

For beam and column elements, concentrated "flexural-rotational" and "axial-flexural-rotational" joints at the two ends of the member are used, respectively. For nonlinear dynamic analyses, the Rayleigh damping model with 5% damping is adopted. The P-Delta effects are also included in the design and analyses of the studied structures.

2.3. Fragility analysis

For fragility analyses, the upper limit of the gravity loads is used for the gravity and lateral load combination according to the following equation [45]:

$$Q_G = Q_D + 0.25Q_L \tag{5}$$

where Q_D and Q_L stand for dead and live loads, respectively (see Fig. 4).

The results of the eigenvalues analysis and the characteristics of the first five vibrational modes for the models are summarized in Table 2. In this table, the parameters T and M represent the vibration period and the effective translational mass coefficient, respectively.

2.4. Fragility analysis using incremental dynamic analysis

In this section, the selected moment-resisting steel structures are first subjected to incremental dynamic analysis (IDA) using probable ground motions. To perform IDA, according to the soil conditions of the site (375 (m/s) $\leq$Vs $\leq$ 750 (m/s)), 20 pairs of accelerograms were selected from the database of PEER website [46].

The selected ground motion records are classified as far-field earthquakes. Among the horizontal components of each earthquake, the component with higher spectral acceleration values in the range of vibrational frequency of the studied structures is selected as the main component (Rm) of the earthquake, while the other component is considered to be secondary (Rn). The utilized accelerograms and characteristics of the main components are listed in Table 3. Since the structures are modeled as 3D, IDA is performed in two perpendicular directions using the main and secondary components of each earthquake simultaneously using the scale coefficient obtained for the main component (see Fig. 7).

In the present study, the Peak Ground Acceleration (PGA (g)) is considered as the intensity measure (IM), while the maximum relative inter-storey drift is selected as the damage measure (DM) for IDA [5]. Fig. 8 demonstrates the IDA curves and the quantitative values corresponding to the different performance levels of the studied structures [47]. The incremental dynamic analysis of 5- and 10-story moment-resisting steel structures includes 473 and 440 separate non-linear time-history analyses, respectively (see Fig. 8). It is obvious that conduction an incremental dynamic analysis (IDA), depending on the number of ground motion records and consecutive scaling until reaching dynamic instability (or any other desired damage limit state), can impose a high computational cost especially in the case of large structural systems.

For the studied moment-resisting steel structures, the fragility curves for the immediate occupancy (IO), life safety (LS), and collapse prevention (CP) performance levels are extracted according to the IM-Based procedure. These curves are demonstrated in Fig. 9.

2.5. Fragility analysis using variable target time (VTT) method

To perform a continuous time analysis, the series of endurance time acceleration functions (in-xyz), titled ETA20inx (01–03) and ETA20iny (01–03) are used [48].

According to Fig. 10, the endurance time analysis is performed by stimulating the structures in two main directions of the plan simultaneously. As shown in this schematic figure, the acceleration amplitude of these accelerograms increases linearly with time.

In order to extract the fragility curves using the endurance time method, the following steps are proposed:

Table 2
Effective mass coefficient and vibration period of the first five vibration modes of the selected moment-resisting steel structures.

Mode No.	5-Storey building			10-Storey building		
	T(s)	M_x (%)	M_y (%)	T(s)	M_x (%)	M_y (%)
1	1.07	0	77.22	1.76	0	73.54
2	1.07	77.22	0	1.76	73.54	0
3	1.06	0	0	1.47	0	0
4	0.38	0.03	13.92	0.68	11.72	0.73
5	0.38	13.92	0.03	0.68	0.73	11.72

Table 3
Characteristics of the main component of utilized accelerograms for IDA.

Record	Earthquake& Year	Station	R[a](km)	Component	M_w	PGA(g)
R_1	Cape Mendocino (US), 1992	Eureka – Myrtle & West	41.97	90	7.1	0.18
R_2	Cape Mendocino (US), 1992	Fortuna – Fortuna Blvd	19.95	0	7.1	0.12
R_3	Cape Mendocino (US), 1992	Loleta Fire Station	25.91	270	7.0	0.26
R_4	Chi-Chi (Taiwan), 1999	TCU070	19.0	E	7.6	0.25
R_5	Chi-Chi (Taiwan), 1999	TCU106	15.0	E	7.6	0.16
R_6	Chi-Chi (Taiwan), 1999	CHY046	24.1	W	7.6	0.19
R_7	Chi-Chi (Taiwan), 1999	CHY041	19.8	N	7.6	0.64
R_8	Chi-Chi (Taiwan), 1999	CHY010	20.0	W	7.6	0.22
R_9	Chi-Chi (Taiwan), 1999	CHY034	15.0	N	7.6	0.30
R_{10}	Chi-Chi (Taiwan), 1999	TCU042	26.31	E	7.6	0.25
R_{11}	Chuetsu-oki (Japan), 2007	Joetsu Ogataku	17.93	NS	6.8	0.32
R_{12}	Darfield (New Zealand), 2010	Heathcote Valley Primary School	24.5	E	7.0	0.63
R_{13}	Iwate (Japan), 2008	Tamati Ono	28.9	NS	6.9	0.28
R_{14}	Iwate (Japan), 2008	Yuzawa Town	25.56	NS	6.9	0.24
R_{15}	Landers (US), 1992	Barstow	34.86	90	7.4	0.13
R_{16}	Loma Prieta (US), 1989	Coyote Lake Dam - Southwest Abutment	20.34	285	6.9	0.48
R_{17}	Northridge (US), 1994	Hollywood – Willoughby Ave	23.07	180	6.7	0.25
R_{18}	Northridge (US), 1994	Lake Hughes #4B - Camp Mend	31.69	90	6.7	0.10
R_{19}	Northridge (US), 1994	Big Tujunga, Angeles Nat F	19.74	352	6.7	0.24
R_{20}	San Fernando (US), 1971	Pasadena – CIT Athenaeum	25.47	90	6.6	0.11

[a] Closest Distance to Fault Rupture.

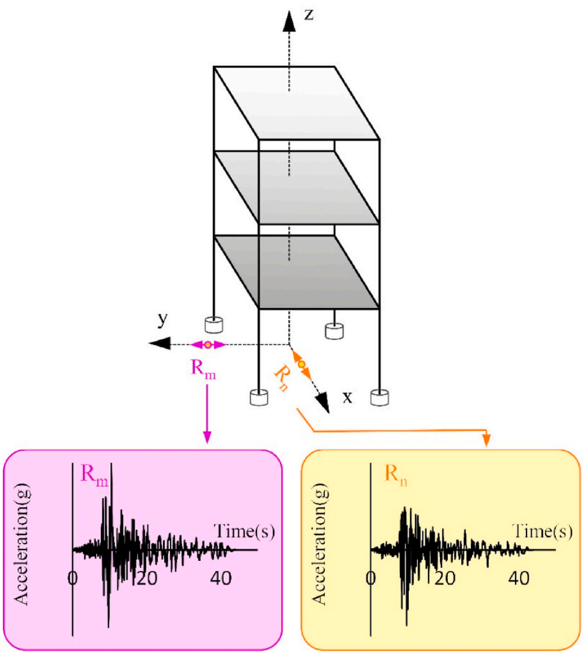

Fig. 7. Two-directional IDA (schematic).

1. As stated earlier, in the endurance time analysis, each instant of time is equivalent to a specified hazard level (see Fig. 11). In the present study, in order to provide the desired statistical space, the initial acceleration functions are scaled using coefficients equal to 0.5, 1 and 1.5. In this case, as shown in Fig. 12, the acceleration spectrum or the scaled ground motion records will be the same at different times. The structures are then analyzed at different times corresponding to different design and maximum probable hazard levels (t_i). Based on the number of considered scaling factors (0.5, 1 and 1.5) and the number of increasing acceleration functions (ETA1, ETA2 and ETA3), nine non-linear dynamic analyses are required to develop the probabilistic estimate of structural response under seismic loading. While the results of this study demonstrate the adequacy of the results in this case, the influence of the selected sample size on the accuracy of the results can be a topic for further studies.
2. By developing acceleration spectra for each accelerogram to the desired time and comparing it with the target site demand spectrum, the equivalent intensity for this time is estimated. Finally, by calculating the mean and the standard deviation of the calculated values, the corresponding intensity for the desired hazard level is presented in an interval. For the selected design hazard

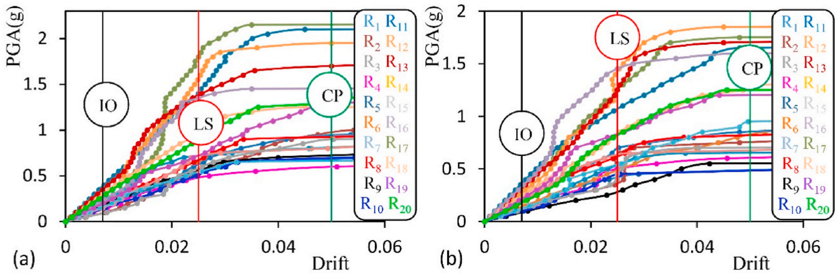

Fig. 8. IDA curves of (a) 5-storey, and (b) 10-storey moment-resisting steel structures.

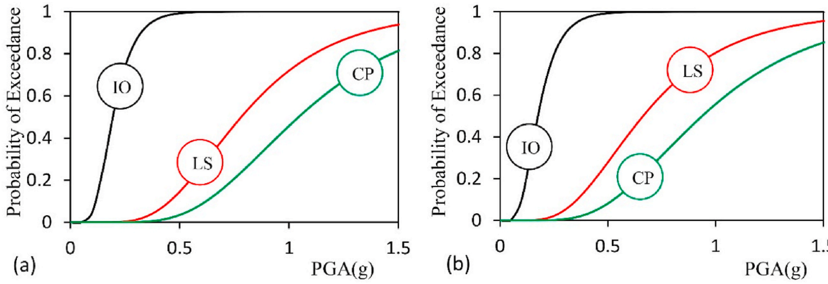

Fig. 9. Fragility curves derived by incremental dynamic analysis for different performance levels: (a) 5-storey, (b) 10-storey moment-resisting steel structures.

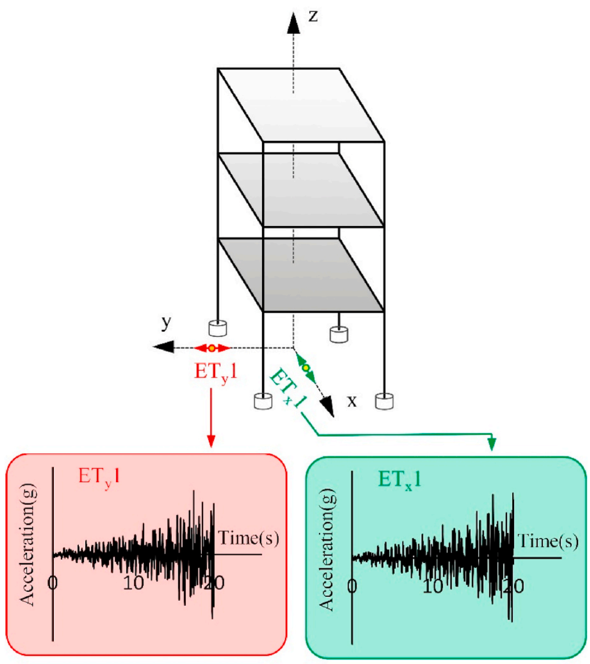

Fig. 10. Two-directional Endurance time analysis of structure (schematic).

level, the acceleration varies between 0.32 g and 0.44 g and the mean value is 0.38 g. For the maximum probable earthquake, these values are increased to 0.53 g, 0.65 g and 0.59 g, respectively.

3. After each analysis, the variations of the storey drift response with time are extracted and the maximum drift response up to the target time corresponding to the desired hazard level (t_i computed in step 1) is recorded (see Fig. 13). In this figure, when the intensity corresponding to a particular damage level is considered, different values of time need to be converted to acceleration or spectral acceleration based on the selected ET record (ETi) and its scale factor (SFi).

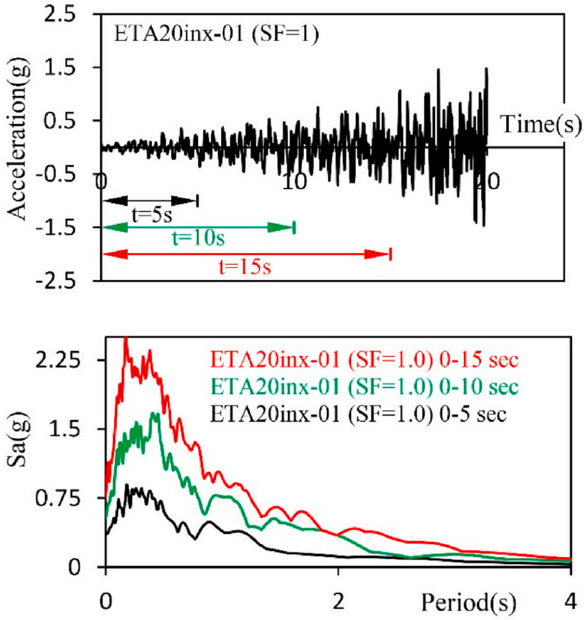

Fig. 11. Acceleration spectrum for increasing accelerograms at different times.

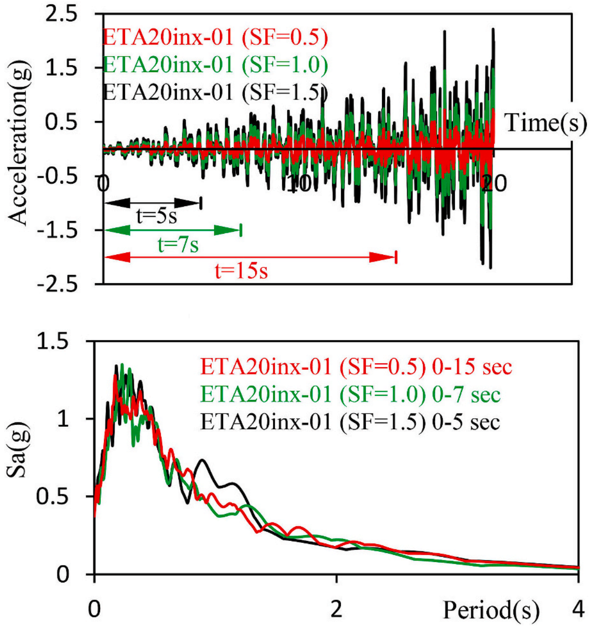

Fig. 12. Acceleration spectrum of scaled increasing accelerograms at times corresponding to a specified level of intensity.

As explained before, changing the target time in the ET method is equivalent to producing an earthquake with a new return period. It means that the frequency content of the earthquake is directly dependent on the selected target time. By scaling the input earthquakes, the target time to reach a specific target response spectrum will also change. For example, Fig. 12 compares the spectra of the first 5, 10 and 15 s of ETA1 record when the scale factors 0.5, 1.0 and 1.5 are respectively utilized (see step 1). It should be noted that the 5s, 10s, and 15s target time values used in this study were selected to cover a range of frequency contents, and hence, provide more reliable results by taking into account the inherited uncertainties in the input earthquakes. While these target values are optional, the results of this study show that they can be efficiently used for practical applications using standard ET increasing acceleration functions.

4. Assuming the log-normal distribution for the calculated values, the probability density function at the desired risk level is

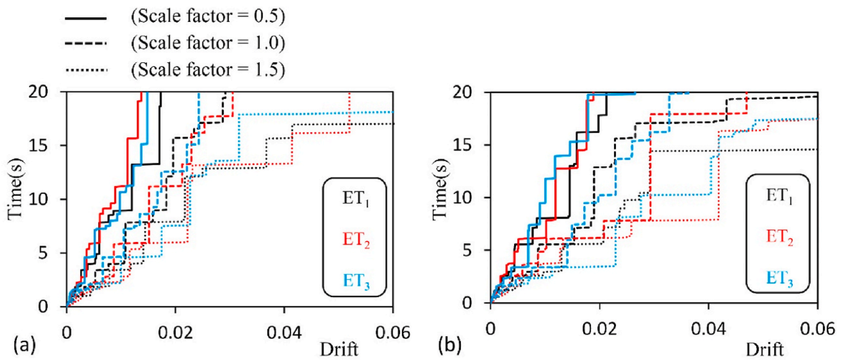

Fig. 13. Maximum storey drifts under scaled increasing accelerograms: (a) 5-storey, and (b) 10-storey moment-resisting steel structures.

extracted. The other steps are the same as those described for the EDP-Based Method in Section 1.1.

For the studied structures and different performance levels, at the design-basis earthquakes (DBE) and the maximum considered earthquakes (MCE), the calculated ranges of the earthquake intensity and the quantities of the exceedance probability are depicted in Fig. 14.

2.6. Accuracy of the results for moment-resisting steel structures

The results of the fragility analyses under the design and the maximum probable hazard levels using variable target time (VTT) and incremental dynamic analysis (IDA) methods are compared in Fig. 15 for the selected moment-resisting steel structures. It is shown that for different performance levels, there is a very good agreement between the results of both methods. In the following, to make a quantitative comparison, at each level of earthquake intensity, the probability of exceeding different performance levels is extracted from the fragility curves depicted in Fig. 15. The extracted values are presented in Table 4.

The results presented in Table 4 indicate that in the 5-storey structure and under both hazard levels, the maximum difference between the results of the two analysis methods for immediate occupancy (IO), life safety (LS), and collapse prevention (CP) performance levels is about 1.5%, 7% and 3.5%, respectively. For the 10-storey structure, the maximum differences for the above-mentioned performance levels are about 1%, 7%, and 5%, respectively. However, it should be noted that the computational time required to perform the endurance time analysis was only 10% of the time required for incremental dynamic analysis.

3. Application of the VTT method for tunnel-from concrete 3D structures

In this section, the efficiency of the proposed variable target time (VTT) method in seismic reliability evaluation of tunnel-from concrete 3D structures is demonstrated using completely different structural systems and earthquake input excitations compared to the previous cases. The VTT method is applied to 5- and 10-storey tunnel-from concrete structures and the reliability results are then compared with the outcomes of fragility analysis based on the conventional IDA.

3.1. Selected tunnel-from concrete structures

The tunnel-from concrete structural system is being increasingly used in industrial mass constructions. This structural system does not include skeletal elements (beam and columns) and instead is composed of wall and slabs elements as the main load carrying components under lateral and gravity loads. The simultaneous casting of walls and slabs in each storey leads to higher integrity (3D performance) and consequently high strength and stiffness of the system [49]. The main reason for the selection of this system for the performance verification of the proposed variable target time (VTT) method is its major differences with the steel moment-resisting frame structures, in terms of material type, elements and connections, strength level, ductility, and finally the overall seismic performance.

The studied structures in this section are based on the models used in Ref. [40] with the regular and symmetric plan shown in Fig. 16. The dashed lines in this figure specify the link beams over the openings (spandrels), which have a length (L_n) and height (h) of 1 and 0.7 m, respectively. To evaluate the effect of structural height, and to be consistent with the models used in the previous section, 5- and 10-storey structures with a storey height of 3 m are considered. These structures are designed according to the ACI 318 standard [50] considering all the requirements of the Building and Housing Research Center for the tunnel-from concrete system [51]. The thickness of the walls in x and y directions are 15 and 22 cm, respectively. Two layers of vertical and transverse reinforcement are utilized in each wall element. All the reinforcing bars in the structures are Ø8 ribbed rebar, except the first four stories of the taller system in which Ø8 ribbed rebar are used. The thickness of the slab is considered to be 15 cm. The “shear wall” elements PERFORM-3D software [44] are used to model the walls and spandrels, while the slabs are modeled using “shell” elements. The concrete compressive strength and steel rebar yield strength values used in the design of the structural components are assumed to be equal to 25 and 400 MPa, respectively. More detailed information about these structures can be found in Ref. [40].

The applied loading, design standard for the seismic performance control of the structures, and the assumptions regarding the site condition and the utilized software for initial design and nonlinear modeling of the system are the same as described in the previous

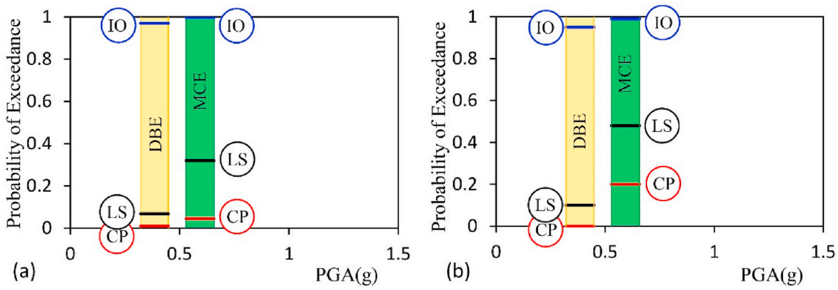

Fig. 14. The fitted fragility curves for different performance levels: (a) 5-storey, and (b) 10-storey moment-resisting steel structures.

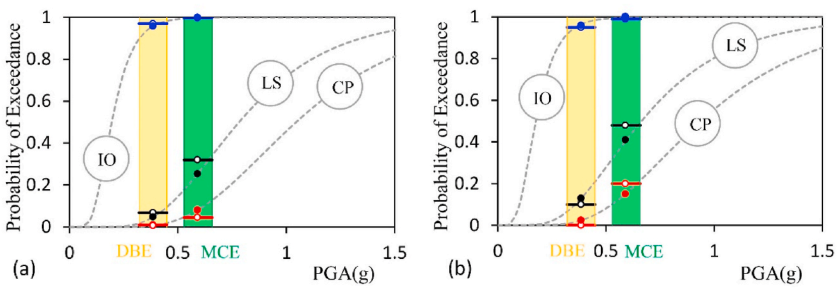

Fig. 15. Comparison of the fragility curves extracted by variable target time (VTT) and incremental dynamic analysis (IDA) methods: (a) 5-storey, and (b) 10-storey moment-resisting steel structures.

Table 4
Exceedance Probability of different performance levels at selected intensity levels.

Structure	Hazard level	Performance levels					
		Immediate Occupancy		Life Safety		Collapse Prevention	
		IDA Method	ET Method	IDA Method	ET Method	IDA Method	ET Method
5-Storey	DBE	95.75	97	4.7	6.8	0.7	1
	MCE	99.7	99.9	25.27	32	8	4.5
10-Storey	DBE	96	95	10	13	2.4	0
	MCE	100	99	41	48	15	20

sections. Due to the interaction of the intersecting walls with slabs, and therefore the 3D performance of the system, the shear force in the walls is considered as the main deformation-control parameter. Considering the free span-to-length ratio of the spandrels ($L_n < h/2$), these members are also modeled as shear-control components. The process of nonlinear modeling of shear behavior in the structural components of this system is discussed in detail in previously published research [52,53], and therefore, for the sake of brevity it is not presented here.

3.2. Fragility analysis of tunnel-from concrete structures using IDA and VTT methods

A set of 12 ground motion records are used for IDA in this section. The utilized records fall in the category of far-fault ground motions with the characteristics listed in Table 5. Based on the relative percentage of the walls in the plan, y direction is identified as the primary direction of the tunnel-form structures for the reliability analyses (see Fig. 16). Accordingly, the main components of the selected ground accelerations are applied to the structures in the y direction.

The proposed VTT method is applied for the selected tunnel-from concrete structures (see Section 2.5). The results are then compared with the fragility curved obtained based on IDA. Fig. 17 demonstrates the derived fragility curves for the studied structures and the quantitative values corresponding to different performance levels [54]. For the studied structures, the fragility curves for the IO, LS and CO performance levels are also obtained as demonstrated in Fig. 18 based on the steps described in the introduction section for IM-based approach (see Section 1).

The tunnel-form concrete structures were then analyzed using the increasing functions and the scale factors as explained in the previous sections. Subsequently, using the proposed variable target time (VTT) method, the probabilities of exceeding different damage states are calculated based on the analysis results for the Design Basis Earthquake (DBE) and Maximum Considered Earthquake (MCE) hazard levels as shown in Fig. 19.

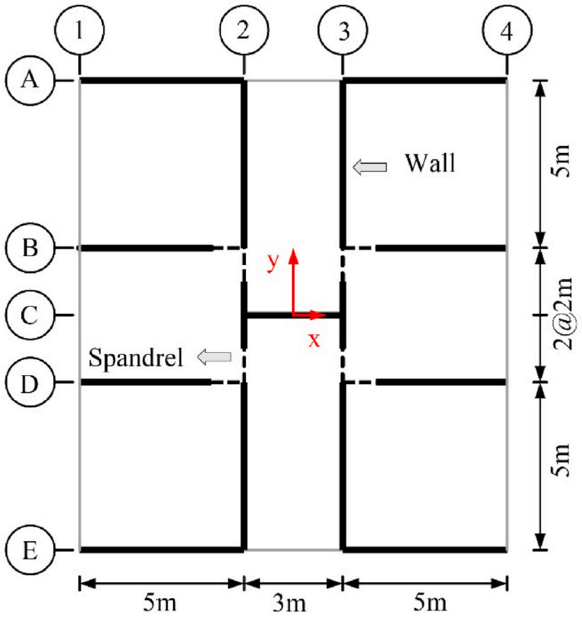

Fig. 16. Plan of the studied tunnel-form concrete structures.

Table 5
Characteristics of the main component of utilized accelerograms for IDA.

Record	Earthquake& Year	Station	R[a](km)	Component	M_w	PGA(g)
R_1	Cape Mendocino (US), 1992	Eureka – Myrtle & West	41.97	90	7.1	0.18
R_2	Cape Mendocino (US), 1992	Fortuna – Fortuna Blvd	19.95	0	7.1	0.12
R_3	Chi-Chi (Taiwan), 1999	TCU045	77.50	90	7.6	0.51
R_4	Friuli (Italy), 1976	Tolmezzo	15.82	0	6.5	0.35
R_5	Hector Mine (US), 1999	Hector	18.66	90	7.1	0.34
R_6	Kobe (Japan), 1995	Nishi-Akashi	16.70	0	6.9	0.51
R_7	Kocaeli (Turkey),1999	Arcelik	53.70	0	7.5	0.22
R_8	Landers (US), 1992	Barstow	34.86	90	7.4	0.13
R_9	Northridge (US), 1994	Hollywood – Willoughby Ave	23.07	180	6.7	0.25
R_{10}	Northridge (US), 1994	Lake Hughes #4B - Camp Mend	31.69	90	6.7	0.10
R_{11}	Northridge (US), 1994	Big Tujunga, Angeles Nat F	19.74	352	6.7	0.24
R_{12}	San Fernando (US), 1971	Pasadena – CIT Athenaeum	25.47	90	6.6	0.11

[a] Closest Distance to Fault Rupture.

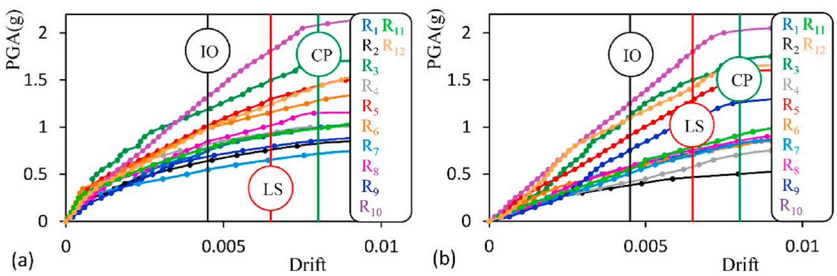

Fig. 17. IDA curves of (a) 5-storey, and (b) 10-storey tunnel-form concrete structures.

3.3. Accuracy of the results for tunnel-form concrete structures

In this section, the fragility curves obtained using IDA and the proposed variable target time (VTT) methods are compared under both DBE and MCE hazard levels, as depicted in Fig. 20. Similar to the previous structures, a very good agreement is observed between the results of the two different approaches. To provide a quantitative comparison, the exceedance probability for different performance levels and under each hazard level are determined from the derived curves and presented in Table 6.

It can be seen from Table 6 that for the 5-storey tunnel-form concrete structure and under both considered hazard levels, the

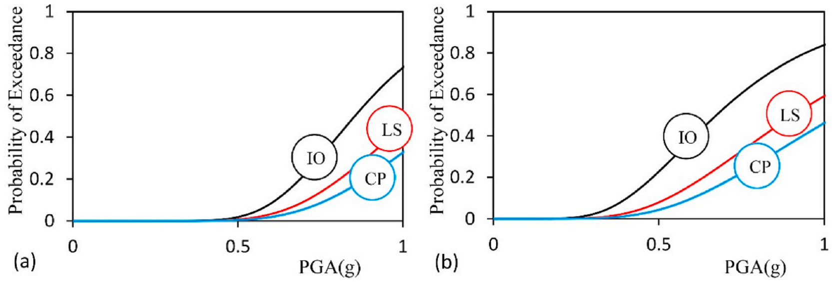

Fig. 18. Fragility curves derived using incremental dynamic analysis for different performance levels: (a) 5-storey, and (b) 10-storey tunnel-form concrete structures.

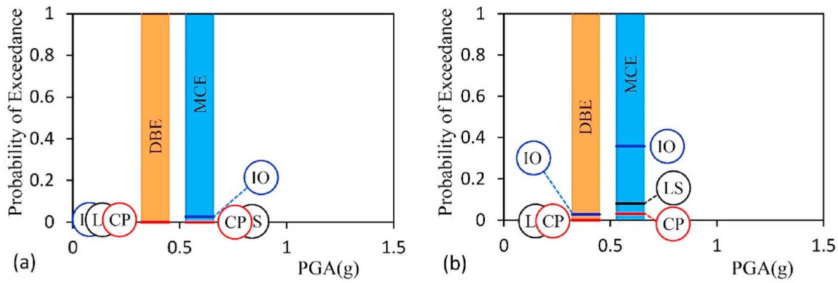

Fig. 19. The fragility curves for different performance levels: (a) 5-storey, and (b) 10-storey tunnel-form concrete structures.

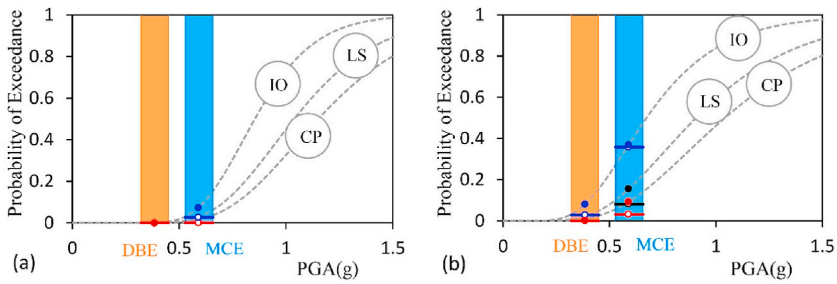

Fig. 20. Comparison of the fragility curves extracted by variable target time (VTT) and incremental dynamic analysis (IDA) methods: (a) 5-storey, and (b) 10-storey tunnel-form concrete structures.

Table 6
Exceedance Probability (%) of different performance levels at selected intensity levels.

Structure	Hazard level	Performance levels					
		Immediate Occupancy		Life Safety		Collapse Prevention	
		IDA Method	ET Method	IDA Method	ET Method	IDA Method	ET Method
5-Storey	DBE	0.0	0.0	0.0	0.0	0.0	0.0
	MCE	7.3	2.6	2.8	0.0	1.6	0.0
10-Storey	DBE	8.0	2.8	2.2	0.0	0.1	0.0
	MCE	36.9	35.8	15.4	8.1	9.2	3.1

maximum difference between the results of the two applied methods for the IO, LS, and CP performance levels are 5.7, 2.8, and 1.6%, respectively. These differences for the 10-storey structure are 5.3, 7.3, and 6.1%, respectively. It should be noted that, considering the number of required non-linear dynamic analyses, the computational time of the VTT method is about 80% less than IDA, which highlights its computational efficiency.

The results of this study, in general, demonstrate the good accuracy of the proposed method in estimating the performance level and exceedance probability for different performance levels at the intensities corresponding to both DBE and MCE, regardless of the adopted lateral load resisting structural system. It is evident that using the variable target time (VTT) method based on the endurance time (ET) analysis can provide acceptable results with significantly lower computational costs. While the results of this study are limited to the considered structures, in general, it can be concluded that the VTT method can be used as a suitable alternative for the conventional incremental dynamic analysis in reliability analysis and development of fragility curves for 3D structures. However, further investigations are required regarding other structural systems considering different geometry and height ranges as well as different intensities and frequency contents for the input excitations, which will be pursued in future studies.

4. Summary and conclusions

In this study, the capability of the recently proposed endurance time method for the development of fragility curves and probabilistic performance evaluations of 3D structures was investigated. The required steps for the development of fragility curves based on IM-Based and EDP-Based methods using conventional incremental dynamic analysis (IDA) were described. Subsequently, a low-computational cost method, called variable target time (VTT) method, was proposed based on the concept of endurance time (ET) analysis to develop the required statistical population and estimate the probabilities for constant hazard levels (EDP-based method) by taking into account the uncertainties associated with the frequency content of the input earthquake records. The fragility curves were then obtained for 5- and 10-storey moment-resisting steel and tunnel-form concrete structures under bidirectional earthquake loadings for different hazard and performance levels using the conventional IDA-based and the proposed ET-based methods. The following conclusions can be made based on the adopted assumption and in the range of studied models:

1. For different performance levels of structures, the fragility curves obtained by the conventional incremental dynamic analysis (IDA) and the proposed variable target time (VTT) methods are in very good agreement. In both moment-resisting steel and tunnel-form concrete structures, the difference between the results for different intensities of input excitation is always less than 7%.
2. Both the conventional and the proposed variable target time (VTT) methods provide similar estimates of the system performance levels under the design-basis earthquakes (DBE) and the maximum considered earthquakes (MCE). However, it is shown that using the VTT can significantly reduce the required computational costs for development of the fragility curves (by 80%) compared to the methods based on incremental dynamic analysis.
3. It is shown that the accuracy of the proposed fragility analysis method based on the endurance time (ET) analyses is not sensitive to the height of the structure and type of the lateral load carrying system. In general, the results of this study demonstrate the good reliability and accuracy of the VTT method as an efficient alternative for the conventional incremental dynamic analysis in reliability analysis and development of fragility curves for 3D structures.

Author contributions

Vahid Mohsenian: *Conceptualization; Methodology; Formal analysis; Investigation; Visualization;* Nima Gharaei-Moghaddam: *Investigation; Resources; Writing - Original Draft.;* Iman Hajirasouliha: *Supervision; Validation; Writing - Review & Editing.*

Declaration of competing interest

The authors declare that they have no known competing financial interests or personal relationships that could have appeared to influence the work reported in this paper.

References

[1] A.H.-S. Ang, W.H. Tang, Probability Concepts in Engineering: Emphasis on Applications to Civil and Environmental Engineering", second ed., vol. 1, Wiley, 2007 the University of Michigan.
[2] V. Mohsenian, I. Hajirasouliha, R. Filizadeh, Seismic reliability assessment of steel moment-resisting frames using Bayes estimators, Struct. Build. (2021), https://doi.org/10.1680/jstbu.20.00211.
[3] F. Zareian, H. Krawinkler, L. Ibarra, D. Lignos, Basic concepts and performance measures in prediction of collapse of buildings under earthquake ground motions, Struct. Des. Tall Special Build. 19 (2010) 167–181, https://doi.org/10.1002/tal.546.
[4] V. Mohsenian, A. Nikkhoo, Evaluation of performance and seismic parameters of eccentrically braced frames equipped with dual vertical links, Struct. Eng. Mech. 69 (6) (2019) 591–605.
[5] D. Vamvatsikos, C.A. Cornell, Incremental dynamic analysis, Earthq. Eng. Struct. Dynam. 31 (3) (2002) 491–514.
[6] V. Mohsenian, A. Mortezaei, Effect of steel coupling beam on the seismic reliability and R-factor of box-type buildings, Struct. Build. 172 (10) (2019) 721–738.
[7] V. Mohsenian, A. Nikkhoo, I. Hajirasouliha, Estimation of seismic response parameters and capacity of irregular tunnel-form buildings", Bull. Earthq. Eng. 17 (9) (2019) 5217–5239.
[8] V. Mohsenian, A. Nikkhoo, A study on the effects of vertical mass irregularity on seismic performance of tunnel-form structural system, Adv. Concrete Constr. 7 (3) (2019) 131–141, 2019.
[9] V. Mohsenian, S. Padashpour, I. Hajirasouliha, Seismic reliability analysis and estimation of multilevel response modification factor for steel diagrid structural systems, J. Build. Eng. (2020), https://doi.org/10.1016/j.jobe.2019.101168.
[10] S. Banerjee, C. Chi, State-dependent fragility curves of bridges based on vibration measurements, Probabilist. Eng. Mech. 33 (2013) 116–125.
[11] V. Mohsenian, R. Filizadeh, Z. Ozdemir, I. Hajirasouliha, Seismic performance evaluation of deficient steel moment-resisting frames retrofitted by vertical link elements, Structures 26 (2020) 724–736.
[12] V. Mohsenian, I. Hajirasouliha, R. Filizadeh, Seismic reliability analysis of steel moment-resisting frames retrofitted by vertical link elements using combined series–parallel system approach, Bull. Earthq. Eng. (2020), https://doi.org/10.1007/s10518-020-01013-9.
[13] M. Grigoriu, Do seismic intensity measures (IMs) measure up? Probabilist. Eng. Mech. 46 (2016) 80–93.
[14] P.S. Koutsourelakis, Assessing structural vulnerability against earthquakes using multi-dimensional fragility surfaces: a Bayesian framework, Probabilist. Eng. Mech. 25 (1) (2010) 49–60.
[15] V.Z. Wang, E. Lyons, Large-sample normal approximation and relevant sensitivity in linear seismic fragility analysis with hierarchically modeled stiffness properties, Probabilist. Eng. Mech. 34 (2013) 91–100.
[16] P. Olmati, F. Petrini, K. Gkoumas, Fragility analysis for the Performance-Based Design of cladding wall panels subjected to blast load, Eng. Struct. 78 (2014) 112–120.

[17] N. Xiang, X. Chen, M.S. Alam, Probabilistic seismic fragility and loss analysis of concrete bridge piers with super elastic shape memory alloy-steel coupled reinforcing bars, Eng. Struct. 207 (2020) 110229.
[18] A. Kalantari, H. Roohbakhsh, Expected seismic fragility of code-conforming RC moment resisting frames under twin seismic events, J. Build. Eng. 28 (2020) 101098.
[19] R. Pang, B. Xu, Y. Zhou, X. Zhang, X. Wang, Fragility analysis of high CFRDs subjected to mainshock-aftershock sequences based on plastic failure, Eng. Struct. 206 (2020) 110152.
[20] H. Liang, J. Tu, S. Guo, J. Liao, D. Li, S. Peng, Seismic fragility analysis of a High Arch Dam-Foundation System based on seismic instability failure mode, Soil Dynam. Earthq. Eng. 130 (2020) 105981.
[21] Z. Wang, N. Pedroni, I. Zentner, E. Zio, Seismic fragility analysis with artificial neural networks: application to nuclear power plant equipment, Eng. Struct. 162 (2018) 213–225.
[22] J. Kiani, C. Camp, S. Pezeshk, On the application of machine learning techniques to derive seismic fragility curves, Comput. Struct. 218 (2019) 108–122.
[23] D. Vamvatsikos, C.A. Cornell, Direct estimation of the seismic demand and capacity of MDOF systems through incremental dynamic analysis of an SDOF approximation, J. Struct. Eng. 131 (4) (2005) 589–599.
[24] S.W. Han, A.K. Chopra, Approximate incremental dynamic analysis using modal push-over analysis procedure, Earthq. Eng. Struct. Dynam. 35 (15) (2006) 1853–1873.
[25] M. Dolsek, P. Fajfar, Simplified nonlinear seismic analysis of infilled reinforced concrete frame, Earthq. Eng. Struct. Dynam. 34 (1) (2007) 49–66.
[26] H. Estekanchi, H. Vafai, Seismic Analysis and Design Using the Endurance Time Method", Volume I: Concepts and Development, Momentum Press, 2018, ISBN 9781947083042, 2018.
[27] H. Estekanchi, H. Vafai, Seismic Analysis and Design Using the Endurance Time Method", Volume II: Advanced Topics and Application, Momentum Press, 2018, ISBN 9781947083264, 2018.
[28] H.E. Estekanchi, A. Vafai, M. Sadeghazar, Endurance Time method for seismic analysis and design of structures, Sci. Iran. 11 (4) (2004) 361–370.
[29] H.E. Estekanchi, K. Arjomandi, A. Vafai, Estimating structural damage of steel moment frames by endurance time method, J. Constr. Steel Res. 64 (2) (2008) 145–155.
[30] M.S. Seif, H. Mehdigholi, H. Estekanchi, M.A. Dastan, Evaluation of seismic behavior of fixed offshore platforms with endurance time method, J. Marine Eng. 15 (2012) 97–103.
[31] H. Hasani, A.A. Golafshani, H.E. Estekanchi, Seismic performance evaluation of jacket-type offshore platforms using endurance time method considering soil-pile-superstructure interaction, Sci. Iran. 24 (4) (2017) 1843–1854.
[32] A. Shirkhani, I.H. Mualla, N. Shabakhty, S.R. Mousavi, Behavior of steel frames with rotational friction dampers by endurance time method, J. Constr. Steel Res. 107 (2015) 211–222.
[33] M.A. Hariri-Ardebili, L. Furgani, M. Meghella, V.E. Saouma, A new class of seismic damage and performance indices for arch dams via ETA method, Eng. Struct. 110 (2016) 145–160.
[34] M.A. Foyouzat, H.E. Estekanchi, Application of rigid-perfectly plastic spectra in improved seismic response assessment by Endurance Time method, Eng. Struct. 111 (2016) 24–35.
[35] A. Guo, Y. Shen, J. Bai, H. Li, Application of the endurance time method to the seismic analysis and evaluation of highway bridges considering pounding effects, Eng. Struct. 131 (2017) 220–230.
[36] J. Bai, S. Jin, J. Ou, Seismic analysis and evaluation of SPSW structural systems by the ET method, J. Constr. Steel Res. 147 (2018) 444–456.
[37] J. Bai, S. Jin, J. Zhao, B. Sun, Seismic performance evaluation of soil-foundation-reinforced concrete frame systems by endurance time method, Soil Dynam. Earthq. Eng. 118 (2019) 47–51.
[38] M. Mashayekhi, H.E. Estekanchi, H. Vafai, S.A. Mirfarhadi, Development of hysteretic energy compatible endurance time excitations and its application, Eng. Struct. 177 (2018) 753–769.
[39] V. Mohsenian, I. Hajirasouliha, A. Nikkhoo, Multi-level response modification factor estimation for steel moment-resisting frames using endurance-time method, J. Earthq. Eng. (2020), https://doi.org/10.1080/13632469.2020.1845875.
[40] V. Mohsenian, N. Gharaei-Moghaddam, I. Hajirasouliha, Seismic performance assessment of tunnel form concrete structures under earthquake sequences using endurance time analysis, J. Build. Eng. 40 (2021) (2021) 102327.
[41] ASCE, Minimum Design Loads and Associated Criteria for Buildings and Other Structures, American Society of Civil Engineers, Reston, Virginia, 2016. ASCE/SEI 7-16.
[42] AISC, Specification for Structural Steel Buildings, American Institute of Steel Construction, Inc, Chicago, IL, 2010. ANSI/AISC 360-10.
[43] Computers, Structures Inc. (CSI, Structural and Earthquake Engineering Software, ETABS, Extended Three Dimensional Analysis of Building Systems Nonlinear Version 15.2.2, 2015. Berkeley, CA, USA.
[44] Computers, Structures Inc. (CSI, Structural and Earthquake Engineering Software, PERFORM-3D Nonlinear Analysis and Performance Assessment for 3D Structures, Version 7.0.0, 2017. Berkeley, CA, USA.
[45] ASCE, Seismic Rehabilitation of Existing Buildings, American Society of Civil Engineers, 2017. ASCE/SEI41-17.
[46] PEER ground motion database, pacific earthquake engineering research center, Web Site: http://peer.berkeley.edu/peer-ground-motion-database.
[47] ASCE, Seismic Rehabilitation of Existing Buildings, American Society of Civil Engineers, 2007. ASCE/SEI41-06.
[48] https://sites.google.com/site/etmethod/et-records.
[49] C. Balkaya, E. Kalkan, Seismic vulnerability, behavior and design of tunnel form building structures, Eng. Struct. 26 (14) (2004) 2081–2099.
[50] ACI Committee 318, Building Code Requirements for Structural Concrete (ACI 318-14) and Commentary, American Concrete Institute, 2014.
[51] BHRCP, Approved technologies indirection of sub-note 2-6, paragraph "D", Note 6, in: A Step in Direction of Building Industrialization, first ed., Building and Housing Research Center Press, 2007, pp. 21–22.
[52] V. Mohsenian, A. Nikkhoo, I. Hajirasouliha, Estimation of seismic response parameters and capacity of irregular tunnel-form buildings, Bull. Earthq. Eng. 17 (9) (2019) 5217–5239.
[53] V. Mohsenian, I. Hajirasouliha, S. Mariani, A. Nikkhoo, Seismic reliability assessment of RC tunnel-form structures with geometric irregularities using a combined system approach, Soil Dynam. Earthq. Eng. 139 (2020) (2020) 106356.
[54] V. Mohsenian, A. Mortezaei, New proposed drift limit states for box-type structural systems considering local and global damage indices, Adv. Struct. Eng. 22 (15) (2019) 3352–3366.